Sensors **2002**, *2*, 436-446

sensors

ISSN 1424-8220

http://www.mdpi.net/sensors

Mathematical Modelling of the Electrode Process of Azithromycin Using Cyclic Voltammetry at Hanging Mercury Drop Electrode

Reyad A. Shawabkeh[1,*] and Maha F. Tutunji[2]

[1] Department of Chemical Engineering, Mutah University, AL-Karak, Jordan. Phone: (962) 6 461-7860 Ext. 3277. E-mail: rshawabk@mutah.edu.jo

[2] Department of Chemistry-University of Jordan, Director of Pharmaceutical Research unit-Royal Scientific Society, Amman, Jordan

* Author to whom correspondence should be addressed.

Received: 9 September 2002 / Accepted: 20 October 2002 / Published: 30 November 2002

Abstract: A theoretical treatment is presented to predict the kinetic behaviour of azithromycin at the surface of hanging mercury drop electrode using cyclic voltammetry. A model is developed to incorporate the occurrence of adsorption of the oxidized and reduced species of azithromycin at the surface of mercury drop electrode. An analytical solution was obtained using MATHEMATICA (V-3, Wolfram Research, Inc.) to predict the cyclic voltammetric profiles by calculating the currents resulting after applying variable potentials ranging –1.9 to –1.3 V versus Ag/AgCl. Simulation runs at different initial concentrations of azithromycin and different scan rates showed good agreement with experimental findings. However, this model should be modified to describe a multilayer adsorption with irreversible electrochemical reaction.

Key words: Adsorption, Azithromycin, Cyclic Voltammetry, Mercury Drop Electrode

Introduction

Macrolide antibiotics are currently gaining prominence in view of their activity in the treatment of various bacterial infections in humans and animals. Generations of macrolide antibiotics such as clarithromycin, roxithromycin and azithromycin are currently used due to their acid stability and wide distribution in tissues.[1-5] Interest in the electrochemical behaviour of active drug constituents has also

been steadily increasing.[6-8] Investigation of electrode processes involving oxidation or reduction reactions may shed more light on in-vivo redox processes.[9, 10] Several researchers have studied the kinetics of electrode processes pertaining to macrolide antibiotics under idealized experimental conditions.[11-14] However, work is still needed to describe the actual redox behaviour of the surface of electrodes. This work is aimed to study the adsorption behaviour of azithromycin on the surface of hanging mercury drop electrode (HMDE) and correlate the in-vitro experimental findings with the theoretical prediction of the suggested process.

Experimental

Chemical and Reagents

A reference standard azithromycin (944 µg/mg, expiration date 2004) was kindly donated by AL Fares Pharmaceuticals, Damascus-Syria. Sodium acetate trihydrate (99.5%, Scharlau, Spain) and acetic acid (99.9% Aristar, BDH-England) were used without further purification. Mercury (99.99%, Fluka-Switzerland) was used after filtration. Methanol was HPLC grade (Romil-England). Deaeration was accomplished by using high purity nitrogen (Air product 99.999%). Deionized water was prepared at the Pharmaceutical Research Unit/ Royal Scientific Society by initiating a reversed osmosis procedure prior to distillation and deionization using an elgacan filter, (C-114 <0.7 µS). Acetate buffer solutions were freshly prepared as a supporting electrolyte (0.1 M, pH 4.64). Stock standard solutions were freshly prepared to contain 1×10^{-2} M of azithromycin dissolved in methanol. The stock solution was used to prepare dilute working standard covering the range 2.5×10^{-5} M to 1.35×10^{-3} M.

Instruments and Apparatus

A 746 Metrohm Electrochemical Trace Analyzer and a 747 VA stand (Metrohm-Herisau-Switzerland). The stand consists of a multi mode electrode (MMD), comprising a Dropping Mercury Electrode (DME), a Static Mercury Drop Electrode (SMDE) and a Hanging Mercury Drop Electrode (HMDE). An Ag/AgCl reference electrode and platinum wire auxiliary electrode completed the three-electrode potentiostat. A universal titration-measuring vessel, which allows working with a total of 5.0 to 10.0 ml volume, was employed. A digital pH-meter (Hi 9321-Hanna) and an analytical balance (AE 2400, Mettler) were also used.

Procedure

Aliquots of stock solutions of azithromycin were individually spiked into the titration vessel containing an acetate buffer solution to make up a total of 10.0 ml volume. Concentrations ranging from 2.5×10^{-5} to 1.35×10^{-3}M were employed. Deaeration was initiated by bubbling high purity oxygen-free nitrogen for 10.0 min through the measuring vessel. Cyclic voltammetry experiments using HMDE were recorded for each of the investigated solutions.

Theory

Generally, the observed reaction mechanism together with the corresponding electrochemical behaviour of macrolide antibiotics, at the surface of the hanging mercury drop electrode (HMDE), may involve a reversible one-electron process. The reactant and the product may *adsorb* at the mercury surface and exists in equilibrium with its corresponding dissolved species as illustrated in the equations 1-a, 1-b, and 1-c.

$$O_{sol\,n} \Leftrightarrow O_{ads} \tag{1-a}$$

$$O + ne^{-} \Leftrightarrow R \tag{1-b}$$

$$R_{sol\,n} \Leftrightarrow R_{ads} \tag{1-c}$$

where: O_{soln} and R_{soln} are the oxidized and reduced species dissolved in the bulk, and O_{ads} and R_{ads} are the oxidized and reduced species adsorbed at the electrode surface, respectively.

The diffusion behaviour of the reactant within the mercury drop is described as

$$\frac{\partial Co(r,t)}{\partial t} = Do\left(\frac{\partial^2 Co(r,t)}{\partial r^2} + \frac{2}{r}\frac{\partial Co(r,t)}{\partial r}\right) \tag{2}$$

where: $Co(r,t)$ is the concentration of reactant at distance r from the center of the mercury drop at time t, and Do is the diffusion coefficient of the reactant within the mercury drop. Similarly, the product, R, diffuses out of the mercury drop; its diffusion may thus be described by

$$\frac{\partial C_R(r,t)}{\partial t} = D_R\left(\frac{\partial^2 C_R(r,t)}{\partial r^2} + \frac{2}{r}\frac{\partial C_R(r,t)}{\partial r}\right) \tag{3}$$

where: $C_R(r, t)$ is the concentration of the reduced species at distance r from the center of the spherical mercury drop and at time t. D_R is the diffusion coefficient of the reduced species within the mercury drop.

To solve equations (2) and (3), the following initial and boundary condition applies:

$$C_O = C_O^* \quad (t = 0,\ r \geq 0) \tag{4}$$

$$C_R = 0 \quad (t = 0,\ r \geq 0) \tag{5}$$

$$D_o\frac{\partial C_O}{\partial r} - \frac{\partial q_O}{\partial t} = -D_R\frac{\partial C_R}{\partial r} + \frac{\partial q_R}{\partial t} \qquad (t > 0,\ r = r_0) \tag{6}$$

$$\frac{C_O}{C_R} = e^{\frac{-nF}{RT}(E-E^O)} \qquad (t = 0,\ r = r_0) \tag{7}$$

$$\lim_{r\to\infty} C_O = C_O^* \quad (t > 0) \tag{8}$$

$$\lim_{r\to\infty} C_R = 0 \quad (t > 0) \tag{9}$$

where C_O^* is the bulk concentration of the reactant initially present, r_o is the radius of the mercury drop, *n is* the number of electrons involved in the reaction, *F* is the Faraday constant, E^o is the formal reduction potential of the reactant, and *E* is the potential of the electrode which can be related to the scan rate, ν, as in equations (10) and (11).

$$E = E_i - \nu t \quad (0 \le t \le t_R) \tag{10}$$

$$E = E_i - 2\nu t_R + \nu t \quad (t \ge t_R) \tag{11}$$

where: E_i is the initial potential of the electrode, and t_R is the time when the scan is reversed to the opposite direction in the cyclic voltammetry. For very low surface concentrations of absorbable ions or molecules, Henry's adsorption isotherm is applied which shows a linear relation between q_o or q_R and the bulk adsorbate concentration *C*. At low concentration levels, the available adsorption sites at the surface will be partially covered. However, at high concentrations, a complete monolayer may be formed. As the bulk concentration of the adsorbates increase, a multilayer may also form. The amount of reactant, q_o, and product, q_R, adsorbed at the surface of the HMDE are related to the solution concentration of the reactant and product, C_o and C_R, respectively. Therefore, any of the isotherm models such as Langmuir's, Fruendlich's, or the Brunauer-Emmett-Teller (BET) model may apply.

Although each of the proposed models can describe the adsorption isotherm, none can perfectly fit the experimentally observed data. If Langmuir's adsorption isotherm is assumed, then equations 12 and 13 hold;

$$q_O = \frac{q_O^s C_O}{(k_o + C_O)} \tag{12}$$

$$q_R = \frac{q_R^s C_R}{(k_r + C_R)} \tag{13}$$

where q_O^s and q_R^s (mole/ cm^2) are the saturation concentrations of the reactant and the product initially present, which cover the monolayer of the electrode surface. The terms k_o and k_r are constants that depend on the electrode potential.

The initial equilibrium conditions can be summarized by equations 14 and 15 as

$$q_O = q_O^* \quad (t = 0,\ r \ge 0) \tag{14}$$

$$q_R = 0 \quad (t = 0,\ r \ge 0) \tag{15}$$

Equations (2) and (3) have been solved using Laplace Transformation and a MATHEMATICA software (v3.0, Wolfram Research, Inc.) to obtain the concentration of the oxidized and reduced species as a function of time and distance from the centre of the mercury drop in accordance with the following:

$$C_O(r,t) = C_O^* + c_1 \frac{e^{-\frac{r^2}{4D_o t}}}{2\sqrt{D_o}\sqrt{\pi} t^{3/2}} + c_2 \frac{\sqrt{D_o} e^{-\frac{r^2}{4D_o t}}}{2r\sqrt{\pi}\sqrt{t}} \tag{16}$$

and

$$C_R(r,t) = c_3 \frac{e^{-\frac{r^2}{4D_R t}}}{2\sqrt{D_R}\sqrt{\pi}t^{3/2}} + c_4 \frac{\sqrt{D_R}e^{-\frac{r^2}{4D_R t}}}{2r\sqrt{\pi}\sqrt{t}} \tag{17}$$

The constant c_1 and c_3 have been evaluated by applying boundary conditions specified in (8) and (9), both were zeros and can thus be eliminated. Equations (16) and (17), however, were substituted into equations (6) and (7) to obtain the following two-non linear equations with c_2 and c_4 as independent variables

$$\frac{1}{c_4\sqrt{D_R}}\left(c_2\sqrt{D_O} + 2r_o C_O^*\sqrt{\pi}\sqrt{t}e^{\frac{r_o^2}{4D_O t}}\right)e^{\frac{(D_O - D_R)r_O^2}{4D_O D_R t}} - e^{\frac{nF}{RT}(E-E_O)} = 0 \tag{18}$$

and

$$\frac{1}{4\sqrt{\pi}r_o^2 t^{3/2}}\left(\begin{array}{l} \dfrac{c_2 e^{-\frac{r_o^2}{4D_o t}}}{\sqrt{D_o}}\left(D_o(r_o^2+2D_o t) + \dfrac{2k_o\pi q_o^* r_o^3(r_o^2-2D_o t)e^{\frac{r_o^2}{2D_o t}}}{\left(c_2\sqrt{D_o} + 2(C_o^*+k_o)r_o\sqrt{\pi}\sqrt{t}e^{\frac{r_o^2}{4D_o t}}\right)^2}\right) - \\ \dfrac{c_4 e^{-\frac{r_o^2}{4D_R t}}}{\sqrt{D_R}}\left(D_R(r_o^2+2D_R t) + \dfrac{2k_r\pi q_R^* r_o^3(r_o^2-2D_R t)e^{\frac{r_o^2}{2D_R t}}}{\left(c_4\sqrt{D_R} + 2r_o k_r\sqrt{\pi}\sqrt{t}e^{\frac{r_o^2}{4D_R t}}\right)^2}\right) \end{array}\right) = 0 \tag{19}$$

At a given time t and scan rate v, equations (10) (11) (18) and (19) have been solved simultaneously to obtain the constants c_2 and c_4. Consequently equations (16) and (17) have been evaluated. The total currents (i_R and i_P), therefore, can be evaluated using equation (20)

$$\frac{i}{nFA} = D_o\left(\frac{\partial C_O}{\partial r}\right)_{r_o} - \frac{\partial q_O}{\partial t} = -D_R\left(\left(\frac{\partial C_R}{\partial r}\right)_{r_o} - \frac{\partial q_R}{\partial t}\right) \tag{20}$$

By substituting the expressions for C_O, C_R, q_O and q_R, the peak currents for the oxidized, i_R, and the reduced species, i_P, at various $E_{1/2}$ values are obtained as

$$i_r = AFn\left[\begin{array}{l} \dfrac{c_2 E^{\frac{r_O^2}{D_O t}} K_O\sqrt{\pi}q_{eO_O}r_o(-r_o+2D_O t)}{2\sqrt{D_O}\left(c_2\sqrt{D_O} + 2E^{\frac{r_O^2}{4D_O t}}(C_{O_o}+K_O)\sqrt{\pi}r_o\sqrt{t}\right)^2 t^{3/2}} - \\ \dfrac{c_2\sqrt{D_0}E^{-\frac{r_o^2}{D_o t}}(-r_o^2+2D_O t)}{4\sqrt{\pi}r_o t^{3/2}} \end{array}\right] \tag{21}$$

and

$$i_p = -AFn\left[\begin{array}{l}\left[\begin{array}{l}E^{\frac{r_o^2}{2D_r t}-\frac{(Ei-Eo)Fn}{RT}} K_r \pi q_e r_o r_o^2 \left[Co_o + \frac{C_2\sqrt{D_o}E^{-\frac{r_o^2}{4D_o t}}}{2\sqrt{\pi}r_o\sqrt{t}}\right]\left(-r_o^2 + 2D_r t\right)\end{array}\right]/ \\ \left[\begin{array}{l}D_r\left[\begin{array}{l}2E^{\frac{r_o^2}{4D_r t}}\left(C_o r + K_r\right)\sqrt{\pi}r_o\sqrt{t} + 2E^{\frac{r_o^2}{4D_r t}-\frac{(Ei-Eo)Fn}{RT}}\sqrt{\pi}r_o \\ \left[Co_o + \frac{C_2\sqrt{D_o}E^{-\frac{r_o^2}{4D_r t}}}{2\sqrt{\pi}r_o\sqrt{t}}\right]\sqrt{t}\end{array}\right]2t - \\ \frac{E^{-\frac{(Ei-Eo)Fn}{RT}}\left[Co_o + \frac{C_2\sqrt{D_o}E^{-\frac{r_o^2}{4D_o t}}}{2\sqrt{\pi}r_o\sqrt{t}}\right]\left(r_o^2 + 2D_r t\right)}{2r_o t}\end{array}\right]\end{array}\right] \quad (22)$$

Results and Discussion

The cyclic voltammograms shown in Figures 1 and 2 illustrate the profiles recorded for low and high concentration ranges obtained at solution pH 4.64. Figure 1 shows cyclic voltammograms that were recorded for 8 successive additions of azithromycin (25 μL each, 1.0×10^{-2} M) to cover the concentration range 2.5×10^{-5} to 2.2×10^{-4} M. These were recorded at a scan rate of 20 V/s. Figure 2, however, illustrates the cyclic voltammograms covering the high concentration range 1.99×10^{-4} to 1.35×10^{-3} M. From the voltammograms, two well-defined cathodic peaks appeared at –1.64 and 0.012 V versus Ag/AgCl. Other anodic peaks were also recorded at –1.79 and –0.18 V versus Ag/AgCl, respectively. As the concentration of azithromycin increases from 2.5×10^{-5} to 7.39×10^{-4}, the cathodic peak at –1.64 V increased. At higher concentration, however, this peak decreased with increasing concentration. This was accompanied by a cathodic shift as illustrated in Figure 2. This observation may be explained by an adsorption process, which takes place at the surface of the mercury drop electrode. At lower concentrations, many active sites are available at the surface of the mercury electrode; as a result peak current was directly proportional to concentration. At higher concentrations, however, the surface of mercury drop became saturated and the total charge flowing during the reduction was thus constant because of the adsorbed azithromycin molecules. The total charge due to diffusion, therefore, continued to increase with concentration, and thus the fraction of the peak current decrease with increasing concentrations.[15-17]

Using the proposed model, profiles of current versus potential (-1.3 to –2.0 V) were generated for fixed azithromycin concentrations of 2.4×10^{-5}, 9.6×10^{-5}, and 1.74×10^{-4}. Figure 3 and Table 1 show the

simulated cyclic voltammograms together with their corresponding adsorption parameters. It appears that as the concentration increased from 2.4×10^{-5} to 9.6×10^{-5}, the cathodic peak current increased linearly from 7μA to 16μA. At higher concentration (~1.74×10^{-4} M), the cathodic peak current sharply increased to 38μA. This could be attributed to a formation of an azithromycin multilayer on the surface of the mercury drop. This necessitates a model replacement of Langmuir's to BET adsorption isotherms. This was authenticated from the values of q_o and q_R, since a dramatic change from 1.0×10^{-8} and 1.0×10^{-9} mole/cm^2 to 1.0×10^{-5} and 1.0×10^{-3} mole/cm^2 were obtained after changing the concentration from 2.4×10^{-5} to 1.74×10^{-4} M.

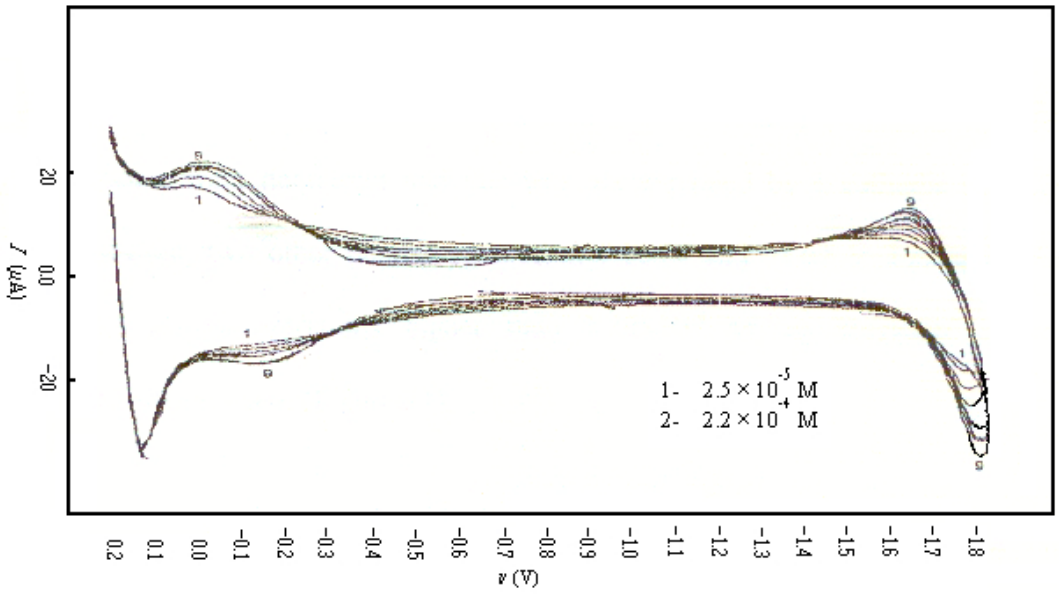

Figure 1. Cyclic voltammograms for the effect of azithromycin concentrations (2.5×10-5–2.2×10-4 M) at the HMDE and a scan rate of 20 V/s.

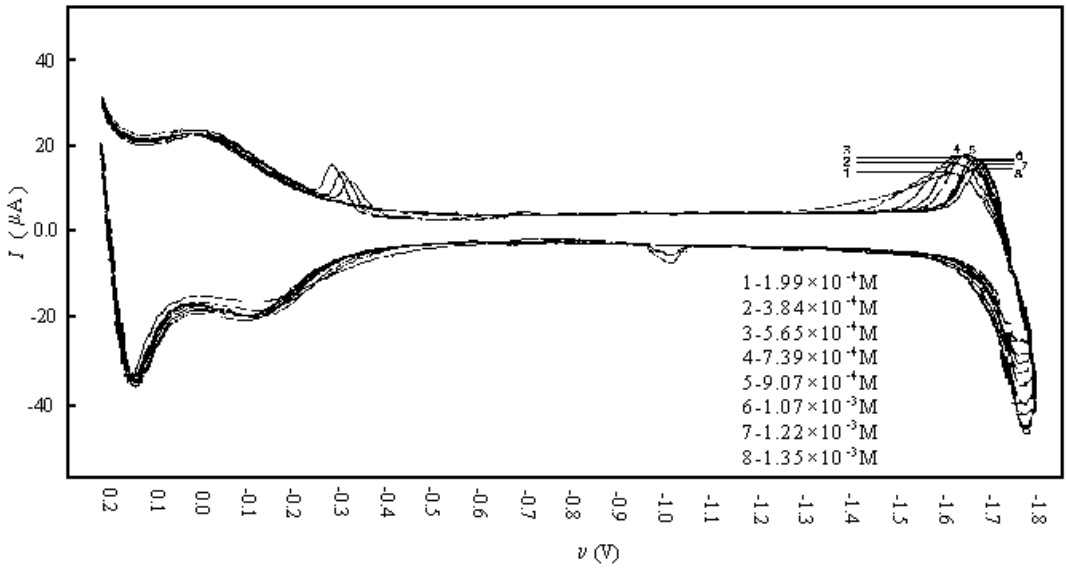

Figure 2. Cyclic voltammograms for the effect of azithromycin concentrations (1.99×10^{-4}–1.35×10^{-3} M) at the HMDE and a scan rate of 20 V/s.

Table 1. Values of Langmuir's model obtained from the simulated model at different initial concentration.

CONCENTRATION (M)	K_O	K_R	q_o (mol/cm^2)	q_R (mol/cm^2)
2.4×10^{-5}	1.0	10	1.0×10^{-8}	1.0×10^{-8}
9.6×10^{-5}	10	10	1.0×10^{-5}	5.0×10^{-3}
1.74×10^{-4}	10	10	1.0×10^{-5}	5.0×10^{-3}

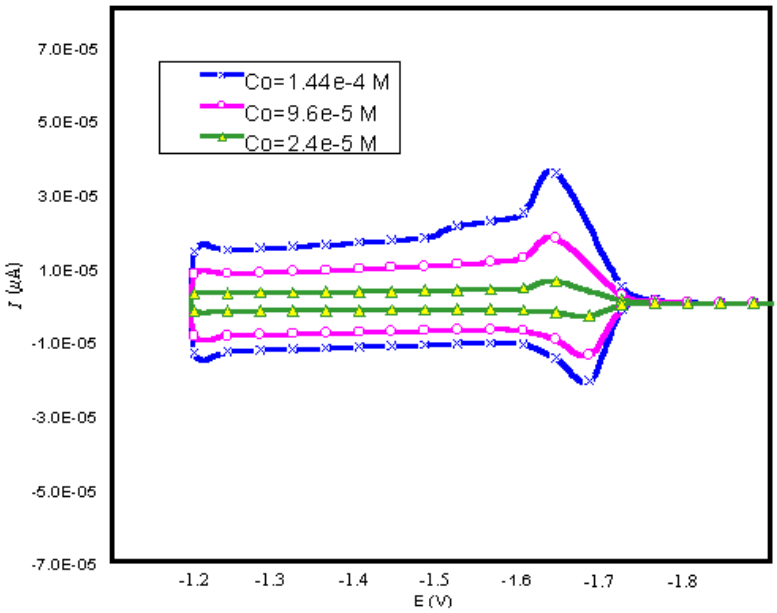

Figure 3. Simulated cyclic voltammograms for the effect of azithromycin concentration obtained at 20V/s.

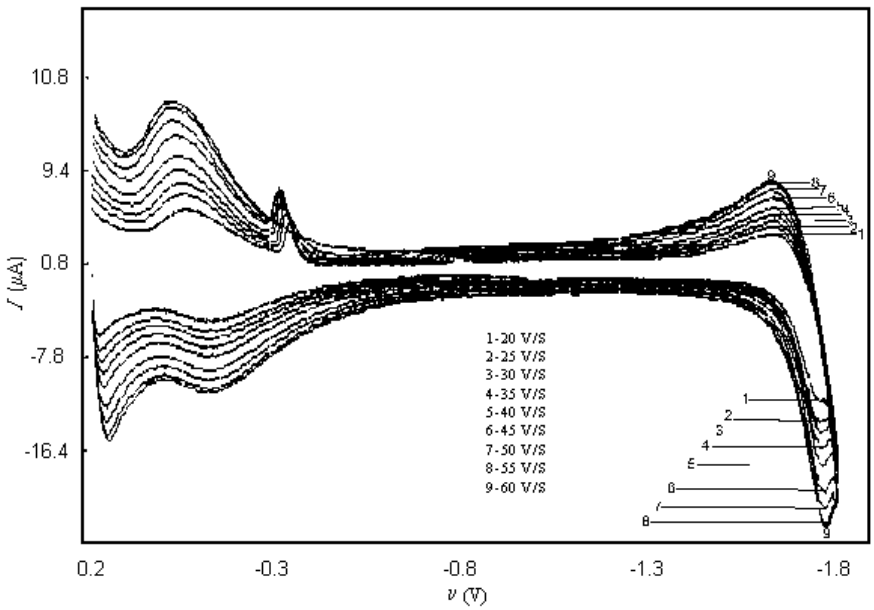

Figure 4. Cyclic voltammograms for azithromycin (1.9×10^{-4} M) obtained at different scan rates.

Figure 4 illustrates the cyclic voltammograms for azithromycin after varying the san rate from 20 to 60 V/s. A difference of 108 mV was observed between the anodic and cathodic potential ($\Delta E = E_{pa} - E_{pc}$) when the scan rate was 20 V/s. This difference was larger for scan rates higher than 20 V/s. The electrochemical reaction may thus be regarded as an irreversible at a scan rate higher than 20 V/s. The observed CV profiles were compared with those simulated from the proposed model at scan rates of 30, 50 and 80 V/s (Figure 5). The proposed model, in contrast, demonstrated a *quasi-reversible* behaviour. Indeed, this is not unexpected since the developed model applies only to described reversible behaviour. Values pertaining to the adsorption isotherm from the simulated model are illustrated in Table 2. These values remained constant after changing the scan rate. This is due to the fact that increasing the scan rate have decreased the time required for the desired amount of azithromycin to get saturated at the surface of the mercury drop, but did not increase that amount per unit surface area of the electrode.

Table 2. Values of Langmuir's model obtained from the simulated model at different scan rates.

SCAN RATE (V/ s)	K_O	K_R	q_o (mol/cm^2)	q_R (mol/cm^2)
30	10	10	1.0×10^{-5}	1.0×10^{-5}
50	10	10	1.0×10^{-5}	1.0×10^{-5}
80	10	10	1.0×10^{-5}	1.0×10^{-5}

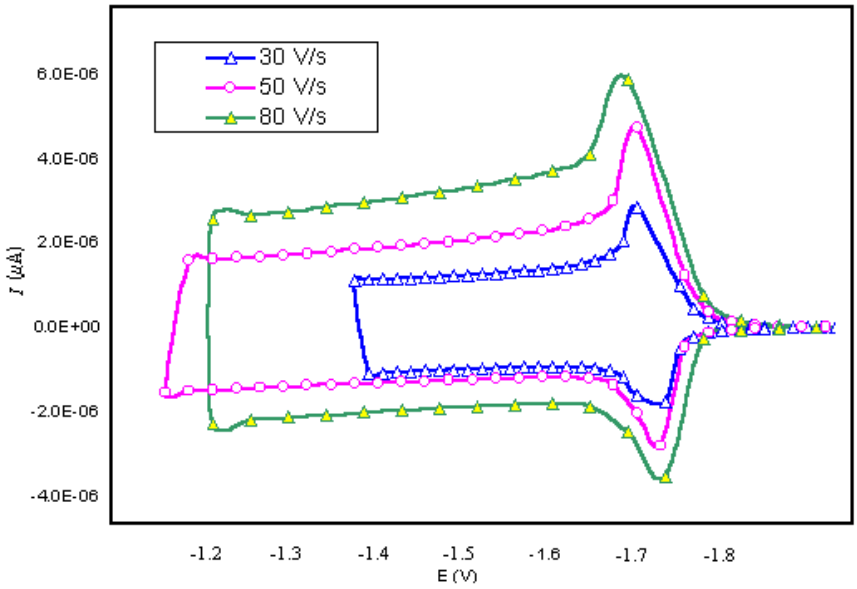

Figure 5. Simulated cyclic voltammograms for azithromycin (1.9×10^{-4} M) at different scan rates.

Notation

A	Surface area of the mercury drop electrode.
C_O^*	Bulk solution concentration of the reactant initially present.
$Co(r,t)$	Concentration of reactant at distance r from the center of the mercury drop at time t.

$C_R(r, t)$ Concentration of the reduced species at distance r from the center of the spherical mercury drop and at time t.

Do Diffusion coefficient of the reactant within the mercury drop.

D_R Diffusion coefficient of the reduced species within the mercury drop.

E Potential of the electrode that can be related to the scan rate.

E_i Initial potential of the electrode.

E^o Formal reduction potential of the reactant.

E_{pa} Anodic peak potential.

E_{pc} Cathodic peak potential.

F Faraday constant.

i_P Peak currents for the reduced species.

i_R Peak currents for the oxidized species.

n Number of electrons involved in the reaction.

q_o Amount of reactant that adsorbed at the surface of the hanging mercury drop electrode.

q_O^s Saturation concentrations of the reactant that is initially present at the surface of the mercury drop.

q_R Amount of the product that adsorbed at the surface of the hanging mercury drop electrode.

q_R^s Saturation concentrations of the product that is initially present at the surface of the mercury drop.

r_o Radius of the mercury drop.

t_R Time when the scan is reversed to the opposite direction in the cyclic voltammetry.

ν Scan rate.

References

1. Gill, C.; Abruzzo, G.; Flattery, A.; Smith, J.; Jackson, J.; Kong, L.; Wilkening, R.; Shankaran, K.; Kropp, H.; Bartizal, K. In vivo evaluation of three acid-stable azalide compounds, L-701,677, L-708,299 and L-708,365 compared to erythromycin, azithromycin and clarithromycin. *The Journal of Antibiotics* **1995**, *48*, 1141-1147.
2. Hoepelman, I.; Schneider, M., Azithromycin: the first of the tissue-selective azalids**.** *International Journal of Antimicrobial Agents* **1995**, 5,145-167.
3. Periti, P.; Mazzei, T.; Mini, E.; Novelli, A., Clinical pharmacokinetic properties of the macrolide antibiotics. Effects of age and various pathophysiological states (Part I). *Clinical Pharmacokinetics* **1989**, *16*, 193-214.
4. Yoshida, H.; Furuta, T., Tissue penetration properties of macrolide antibiotics--comparative tissue distribution of erythromycin-stearate, clarithromycin, roxithromycin and azithromycin in rats. *The Japanese Journal of Antibiotics* **1999**, *52*, 497-503.
5. Turcinov, T.; Pepeljnjak, S., Azithromycin potency determination: optimal conditions for microbiological diffusion method assay. *Journal of Pharmaceutical and Biomedical Analysis* **1998**, *17*, 903-910.

6. Gandhi, R.; Kaul, C.; Panchagnula, R., Validated LC method for in-vitro analysis of azithromycin using electrochemical detection. *Journal of Pharmaceutical and Biomedical Analysis* **2001**, *23*,1073-1079.
7. Molina, M.; Serna, C.; Lopez-Tenes, M.; Chicon, R., Derivation of a general theory for reversible multistep electrode processes in voltammetry with constant potential at spherical electrodes. *Electrochemistry Communications* **2000**, *2*, 267-271.
8. LaCourse, W.; Owens, G., Pulsed electrochemical detection of thiocompounds following microchromatographic separations. *Analytica Chimica Acta* **1995**, *307*, 301-319.
9. Meulemans, A., Electrochemical detection of nitroso-arginine as an intermediate between N-hydroxy-arginine and citrulline. An in vitro versus in vivo study using microcarbon electrodes in neuronal nitric oxide synthase and mice brain. *Neuroscience Letters* **2000**, *294*, 125-129.
10. Wallman, L.; Levinsson, A.; Schouenborg, J.; Holmberg, H.; Montelius, Z.; Danielsen, N.; Laurell, T., Perforated silicon nerve chips with doped registration electrodes: in vitro performance and in vivo operation. *IEEE Transactions on Bio-Medical Engineering* **1999**, *46*,1065-1073.
11. Abo El-Maali, N., Electrochemical behaviour of the monobactam antibiotic aztreonam at different electrodes and in biological fluids, Bioelectrochemistry and Bioenergetics **1998**, 45, 281-286.
12. Shen, D.; Huang, M.; Chow, L.; Yang, M., Kinetic profile of the adsorption and conformational change of lysozyme on self-assembled monolayers as revealed by quartz crystal resonator. *Sensors and Actuators B: Chemical* **2001**, *77*, 664-670.
13. Di Natale, C.; Giampaolo, C.; D'Amico, A., Study of the noise in adsorption-desorption phenomena using the Allan variance and a quartz microbalance. *Sensors and Actuators B: Chemical* **2000**, *65(1-3)*, 227-231
14. Apostolakis, J.; Georgiou, C.; Koupparis, M., Use of ion-selective electrodes in kinetic flow injection: determination of phenolic and hydrazino drugs with 1-fluoro-2,4-dinitrobenzene using a fluoride-selective electrode. *The Analyst* **1991**, *116*, 233-237.
15. Rong, C.; Anson, F., Unusual strong adsorption of high charged heteropolytungstate anions on mercury electrode surfaces. *Analytical Chemistry* **1994**, *66*, 3124-3130.
16. Wopschall, R.; Shain, I., Effect of adsorption of electroactive species in stationary electrode polarography. *Analytical Chemistry* **1967**, *39*, 1514-1527.
17. Hanewinkel, C.; Winkes, H.; Schumacher D.; Otto A, Adsorption of metal cations precisely quantified by surface resistance of thin epitaxial silver film electrodes. *Electrochimica Acta* **1997**, *42*, 3345-3349.

Sample Availability: Available from the authors.